3.3 μm interband-cascade resonant-cavity light-emitting diode with narrow spectral emission linewidth

Daniel Díaz-Thomas, Oleksandr Stepanenko, Michaël Bahriz, Stéphane Calvez, Thomas Batte, Cyril Paranthoen, Gilles Patriarche, Eric Tournié, Alexei Baranov, Guilhem Almuneau, et al.

published in Semiconductor Science and Technology
https://doi.org/10.1088/1361-6641/abbebc

3.3 µm interband-cascade resonant-cavity light-emitting diode with narrow spectral emission linewidth

D.A. Díaz-Thomas[1], O. Stepanenko[2], M. Bahriz[1], S. Calvez[2], T.Batte[3], C. Paranthoen[3], G. Patriarche[4], E. Tournié[1], A.N. Baranov[1], G. Almuneau[2], C. Levallois[3], and L. Cerutti[1]

[1] IES, Univ. Montpellier, CNRS, F-34000 Montpellier, France

[2] LAAS-CNRS, Université de Toulouse, CNRS, 7 Avenue du Colonel Roche, 31400, Toulouse, France

[3]Univ Rennes, INSA Rennes, CNRS, Institut FOTON – UMR 6082, F-35000 Rennes, France

[4] C2N, CNRS- Univ. Paris-Sud, Univ. Paris-Saclay, 10 Avenue Thomas Gobert, F-91120 Palaiseau, France

E-mail: laurent.cerutti@umontpellier.fr ; daniel.diaz-thomas@umontpellier.fr

Received xxxxxx

Accepted for publication xxxxxx

Published xxxxxx

Abstract

https://doi.org/10.1088/1361-6641/abbebc

We demonstrate an Interband Cascade Resonant Cavity Light Emitting Diode (IC-RCLED) operating near 3.3 μm at room temperature. The device is composed of a Sb-based type-II interband-cascade active zone enclosed between two distributed Bragg mirrors (DBR). The bottom high reflective DBR is composed of GaSb/AlAsSb quarter-wave layers. A metamorphic III-As region is grown after the active zone to benefit from the AlOx technology for efficient electro-optical confinement. The structure is finished with a top ZnS/Ge dielectric DBR. The devices with oxide aperture ranging from 5 to 35 μm were studied in the continuous wave (CW) regime. The fabricated IC-RCLEDs operated up to 80°C (set-up limited) and exhibited narrow emission spectra with a full width at half maximum (FWHM) of 21 nm, which is 20 times smaller compared with conventional IC-LEDs. The narrow emission line and its weak temperature dependence make the fabricated devices very attractive for low cost gas sensors.

Keywords: RCLED, midinfrared, interband-cascade

1. Introduction

The strong absorption of hydrocarbons and other pollutants in the window of atmospheric transparency between 3 and 4 μm makes this spectral region very attractive for environmental monitoring [1]. Sb-based semiconductor light sources allow addressing such gas sensing applications in the mid-infrared (mid-IR). Over the last decade, significant progress has been achieved in mid-IR emitters employing Interband Cascade (IC) structures based on InAs/GaInSb type-II quantum wells, particularly efficient in the 3 - 4 μm range [2]. The luminescence of the IC active region enables both TE and TM light polarizations and therefore the ability to vertically extract the light from a planar cavity structures such as light emitting diodes (LEDs) [3], or vertical cavity surface emitting lasers (VCSELs) [4]. Resonant Cavity Light Emitting Diodes (RCLEDs) are attractive for the development of low-cost systems for gas analysis [5] Due to a narrower emission linewidth [Sarcan F, Wang Y, Krauss T F, Erucar T, and Erol A 2020 *Optics and Laser Technology* **122** 105888] such sources can offer better overlap with absorption features of

the analyzed specie compared with the conventional LEDs and thus improved sensitivity [Al-Saymari F A, Craig A P, Lu Q, Marshall A R J, Carrington P J, and Krier A 2020 *Optics Express* **28** 23338]. Usually, there is only one DBR in RCLEDS, placed below the active region. A simpler Bragg mirror with a few quarter-wavelength dielectric layers deposited on the top of an RCLED structure is however useful to control the device properties. By adjusting its reflectivity the RCLED emission linewidth can be matched with the shape of the desired absorption band making their relative overlap to be little sensitive to measurement conditions and hence no sophisticated control is needed to compensate the eventual change. In the case of a VCSEL, the wavelength of the narrow laser emission line should be precisely fixed inside the absorption band to avoid signal fluctuations or scanned around it, which requires specific electronic circuits resulting in elevated equipment cost. The main motivation of this work was to develop light sources for specific spectroscopic applications which require an emission linewidth intermediate between that of conventional LEDs (few tens nm) and VCSELs (< 1 nm).

Since their first demonstration in 1992 [6], only a few mid-IR RCLEDs, based on arsenide [7], phosphide [8] and antimonide compounds have been reported [9] [10], with only one IC-RCLED operating at RT [11]. Even if RCLEDs use less distributed Bragg reflectors (DBR) pairs than VCSELs, their electrical resistivity can induce a strong self-heating of the devices [12] and lead to a degradation of the performances. The use of an intracavity electrical contact has been proposed and successfully demonstrated in VCSELs [13-15] to circumvent this issue. In addition, in a RCLED, the current is commonly [11] injected through an annular anode contact pad leading to a non-negligible radial

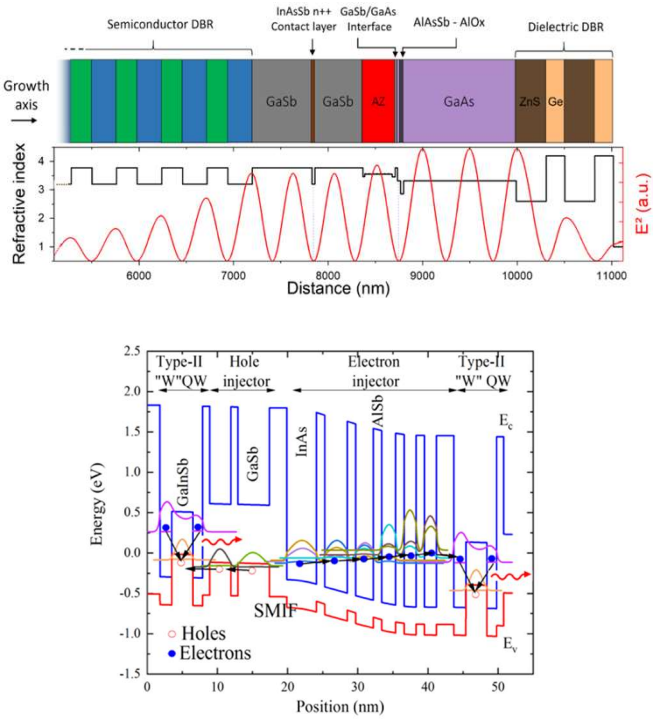

Figure 1. a) Scheme of the IC-RCLED structure with the refractive index profile (black) and the EM intensity distribution (red).
b) Energy band diagram of one stage of the active region simulated with Nextnano©, showing the cascade process.

inhomogeneity. Even though several strategies used for Sb-based VCSELs such as a buried tunnel junction [13], or an underetched tunnel junction [14] can be implemented in RCLEDs, these technologies are still very complex. A simpler solution would be to implement the lateral electro-optical confinement oxide-based technology [15] conventionally used in commercial near infrared GaAs VCSELs. This process has been successfully demonstrated on InP [16] and GaSb VCSELs [15] which exploit a metamorphic growth and a selective thermal oxidation of an AlGaAs layer on top of the active region. Moreover, it has been shown that the lateral confinement may contribute to high emission efficiencies and narrow linewidth in RCLED devices [17].

In this article, we describe the fabrication of IC-RCLEDs emitting at 3.3 µm, with GaSb/AlAsSb and ZnS/Ge bottom and top DBRs, respectively. To reduce the series resistance, we used vertical structure with intracavity contacts and a GaAs/AlGaAs metamorphic region above the IC active zone. Finally, we report on the performances of this metamorphic aperture-confined IC-RCLED which operates at high temperature in CW providing narrow emission spectra in comparison to conventional IC-LED.

2. Experimental details

2.1 IC-RCLED design and epitaxy

Figure 1.a) depicts a schematic diagram of the IC-RCLED structure and the intrinsic optical field standing wave intensity distribution at the targeted emission wavelength (3.3 µm). The RCLED is composed of a semiconductor part: the lower DBR, the cavity followed by the arsenide section for lateral onfinement. This bottom part of the RCLED structure is capped with a dielectric top DBR. The semiconductor-based section was grown by molecular beam epitaxy (MBE) in a RIBER Compact 21E solid source system equipped with As- and Sb- valved cracker cells.

The growth was performed on a 2-inch (100)-oriented N-doped GaSb substrate. Different growth temperatures were applied across the structure to ensure the good quality of the IC gain section [18]. The temperature was measured with an optical pyrometer calibrated using the (1x3) to (2x5) reconstruction change of GaSb. The surface oxide of the substrate was thermally desorbed around 550°C under Sb2 overflow in order to prevent the Sb desorption from GaSb. The growth was started with a low N-doped ($1x10^{17}$ cm-3) GaSb buffer layer followed by the bottom DBR grown at a substrate temperature of

510 °C. This DBR is composed of 14 pairs of quarter-wave GaSb and $AlAs_{0.08}Sb_{0.92}$ layers with a refractive index contrast of Δn~0.6 enabling a maximum reflectivity seen from the cavity as high as 96 % omitting the residual losses. Despites this high reflectivity, it is still half of the number of DBR pairs required for VCSEL structure [13]. The optical losses are however considered to be weak since free-carrier absorption phenomena have been limited by using low N-doped materials in this part of the structure ($1x10^{17}$ cm^{-3}) [19]. The 3-λ-thick optical cavity consists of a ~1 µm thick N-doped GaSb layer (5.10^{17} cm^{-3}), a 7-stage IC active zone, and a metamorphic N-doped AlGaAs/GaAs region. A 30-nm-thick heavily N-doped $InAs_{0.92}Sb_{0.08}$ layer ($n = 3×10^{18}$ cm^{-3}) is inserted at the first node of the internal optical field in the cavity, in the middle of the 1-µm-thick GaSb bottom layer, to serve as the bottom intracavity N-contact layer. ~~The 7-stage IC active zone designed with carrier rebalancing.~~ The Figure 1.b) shows the energy band diagram of one stage of the IC active region simulated with Nextnano© software [See www.nextnano.com/index.php for "Nextnano GmbH - semiconductor software solutions."]. It consists of a "W" type-II QWs where the

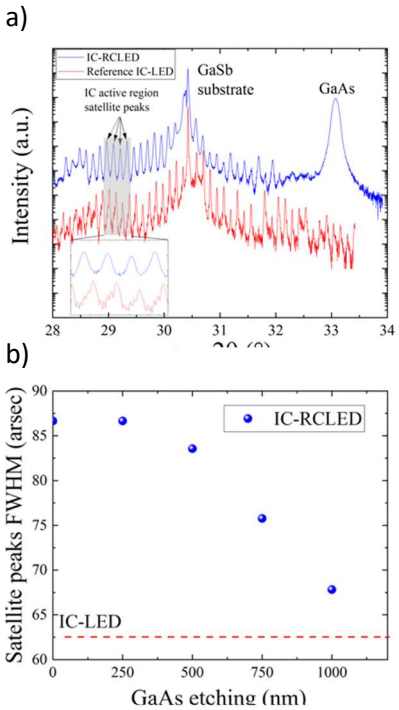

Figure 2. a)- ω -2θ HRXRD scans at the (0 0 4) reflection for the RCLED and reference LED structure. *Inset:* magnification on the satellite peaks – b) Evolution of the FWHM of the satellite peaks of the RCLED with etched GaAs.

interband transition takes place following by the hole injector. Then, the GaSb/InAs semi-metallic interface (SMIF), where the electron in the valence band make their transition in the conduction band. This tunnel junction is mitigated by an AlSb layer to reduce parasitic interband absorption. Finally the electron injector is composed with a serie of alternating AlSb barriers and InAs wells with graded thickness to compensate the applied field and allows to inject the electrons in the next stage. Several InAs layers of the electron injector are n-doped at 4.5 10^{18} cm^{-3} for carrier rebalancing [20]. More details on the physic of IC active region and

interband cascade laser can be found elsewhere [2 ; Vurgaftman I, Bewley W W, Canedy C L, Kim C S, Kim M, Lindle J R, Meritt C D, Abell J, and Meyer J R 2011, *IEEE Journal of Selected Topics in Quantum Electronics* **17** 1435]. The active region is grown at 435°C [11], and is sandwiched between 2 transition layers composed of graded InAs/AlSb superlattices in order to smooth the voltage drop between the GaSb layers and the active region. The active zone is designed to exhibit resonant periodic gain at the target wavelength of 3.3 µm. Then, a metamorphic GaAs layer (25 nm) is grown, with the GaSb/GaAs interface placed at the 1st internal optical field node above the active zone in order to minimize the optical losses related to the high density of dislocations created by the large lattice mismatch between GaSb and GaAs (□a/a~8%). A 20-nm-thick $Al_{0.98}GaAs$ layer is grown next to this interface to implement, upon oxidation as conventionally used in AlGaAs/GaAs VCSEL, the electrical confinement necessary for the lateral control of the current. It is also intended to reduce surface recombinations on mesa edges, which are usually high on GaSb [15] [16], [21], [22]. This layer is capped by a 1-µm-thick N-doped (1.10^{18} cm-3) GaAs spreading layer to ensure uniform current injection. The entire metamorphic part of the structure was grown at 435°C, a relatively low-temperature in GaAs-based standards, but such a low temperature is required to avoid degradation of the IC active zone caused by atomic intermixing at the interfaces [18]. To compare the structural and the optical properties of this IC-RCLED, a reference IC-LED containing the same active region capped with 200 nm of n-type GaSb was also grown.

2.2 Structural and optical characterizations

The crystalline quality of the grown structures was characterized by high-resolution X-ray diffraction (HR-XRD). The experimental ω-2θ patterns measured on the (004) reflection are shown on Fig. 2. The diffractogram depicted in Figure 2.a shows for the RCLED structure, a larger peak appears at higher angles corresponding to the fully relaxed GaAs layer.

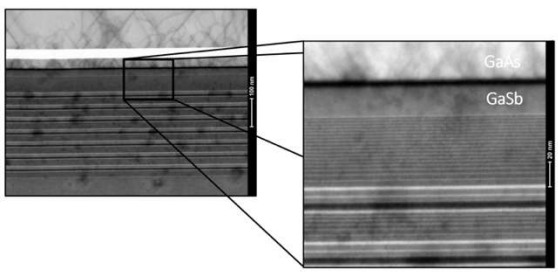

Figure 3. Transmission electron microscopy cross-section views of the RCLED showing dislocations propagating above the GaSb/GaAs metamorphic interface

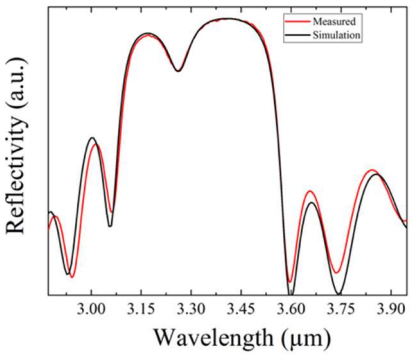

Figure 4. Experimental and simulated top reflectivity spectrum of the RCLED epitaxial structure without the top dielectric DBR.

Moreover, both structures display a series of satellite peaks up to the 16th order arising from the periodic IC active zone. ~~The thickness of the IC active region extracted from the angle separation between the satellite peaks is 41.2 nm, in good agreement with the target value of 41.5 nm~~. The inset in the Figure 1.a) shows that the satellite peaks for the RCLED are however observed to be larger than those of the conventional IC-LED. This could be attributed to the X-ray scattering within the metamorphic GaAs layer because of the high density of dislocations. ~~arising at the GaSb/GaAs interface~~. To confirm this hypothesis, the top GaAs was dry etched using inductively coupled plasma reactive ion etching (ICP-RIE) on a part of the sample.

Four etching steps of 250 nm each were performed and HRXRD was carried out between each step. Figure 2.b displays the evolution of the full width half maximum (FWHM) averaged over the 10 satellite peaks closest to the substrate peak.

Upon removal of the GaAs layer, the FWHM of the satellite peaks from the IC-RCLED approaches the value of the reference IC-LED. Furthermore, the effect of these dislocations on the active zone of the device was studied using transmission electron microscopy (TEM). Figure 3 clearly demonstrates that the dislocations do not extend from the GaAs/GaSb interface down to the active region, contrarily to what it was observed in metamorphic GaAs/InP structures [23], and remain confined to the arsenide layers.

Calculated and measured top optical reflectance spectra of the RCLED epitaxial structure are presented in Figure 4. The measurement was performed with a Brucker FTIR spectrometer under quasi-normal incidence. The stop-band is centered at 3.32 μm and the reflectivity dip related to the cavity resonance is at 3.26 μm. This wavelength detuning from 3.3 μm is attributed, based on reflectivity calculation, to a cavity thickness of about 3% smaller than the target value.

2.3 Devices fabrication

The epitaxial wafer was patterned with circular mesas with diameters ranging from 25 µm to 55 µm using standard optical photolithography and a combination of ICP-RIE and wet etching. The mesas were etched down to the InAsSb bottom contact layer. After this step, a thermal selective lateral oxidation process of the Al-rich AlGaAs layer was performed at temperature at conditions similar to those used for AlGaAs/GaAs structures reported in [21] [24]. The progress of the oxidation front was observed during the oxidation process with a real-time in situ monitoring optical system [25]. After oxidation, the aperture diameters spanned from 5 to 35 µm incremented by 2 µm.

This step was followed by surface passivation of the structures using a Si_3N_4 ICP-PECVD coating and then Ti/Au metallization of the InAsSb layer for the bottom contact. Afterwards, contact pads for top contacts and another Si_3N_4 passivation layer were deposited.

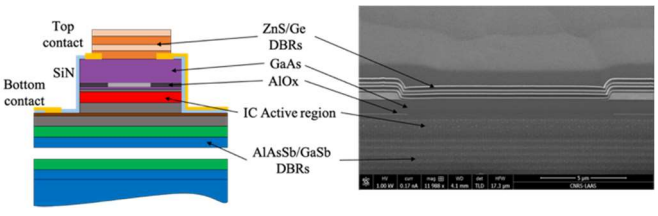

Figure 5. Schematic and Scanning Electron Microscopy (SEM)picture of a cross section of the IC-RCLED after processing

Finally, a two-pair ZnS/Ge dielectric Bragg mirror was deposited by RF sputtering and patterned by a lift-off process. The reflectivity seen from the cavity is calculated to be around 91%, a value slightly lower than the bottom DBR allowing a better extraction of the light. Figure 5 shows a schematic and a SEM cross section image of the complete RCLED structure at the end of the process flow. The oxide confinement aperture is clearly visible in Figure 5 and is of the same size as the top emission window defined by the contact ring, which ensures an efficient current confinement. In parallel, the IC-LED (without lateral confinement) was processed with mesa diameters of 100 µm and ring contacts width of 20 µm.

2.4 Electro-optical characterizations

Electro-optical measurements of the fabricated devices were performed under CW operation using a thermoelectrically-controlled stage. Figure shows the CW P-I-V characteristics at 20°C for different oxide aperture diameters. The turn-on voltage for all IC-RCLEDs at 20°C is around 4.5 - 5 *V*, which is higher than the expected value for the IC active region (N x E_g)

and may be attributed to the GaSb/GaAs junction or to a low performance of the contact on the metamorphic GaAs layer. The optical power increases with the devices aperture. It varies between 9 µW at 9 mA to 60 µW at 36 mA, for the 5 and 35 µm aperture diameter, respectively. As presented in the Figure 6.b), when the aperture diameter increases from 5 to 35 µm, the differential series resistance decreases from 115 to 10 Ω , on a par with values obtained for oxide-apertured GaAs VCSELs [26] and mid-IR-emitting implanted InP VCSELs [27] demonstrating efficient lateral electrical confinement. This parameter was fitted using $R_s=R_L+R_v$ where R_L is lateral resistance, $R_L=\rho_L/(\pi D_a)$ and the vertical resistance $R_V = 4\rho_V/(\pi D_a^2)$, and lead to ρ_L ~1200 Ω.µm and ρ_V ~1000 Ω.µm^2.

Figure 6.c), shows the electroluminescence spectra (EL) in CW and at 20°C of the 35 µm IC-

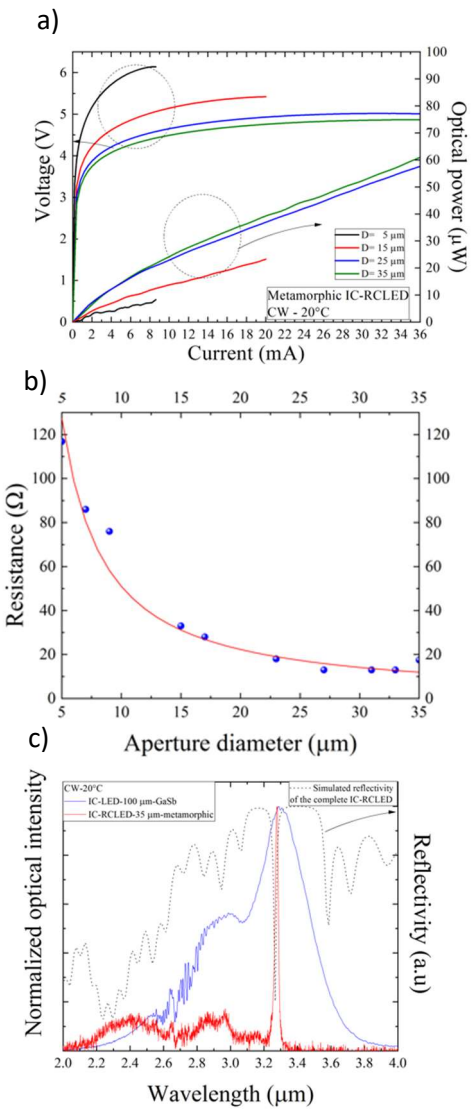

Figure 6. (a) CW L – I – V characteristics, and (b) series resistance for RCLEDs as a function of the aperture diameter ranging from 5 μm to 35 μm. (c) Emission spectra of a 35 μm oxide aperture IC-RCLED and 100 μm mesa diameter IC-LED at 20°C in CW and simulated reflectivity of the whole IC-RCLED

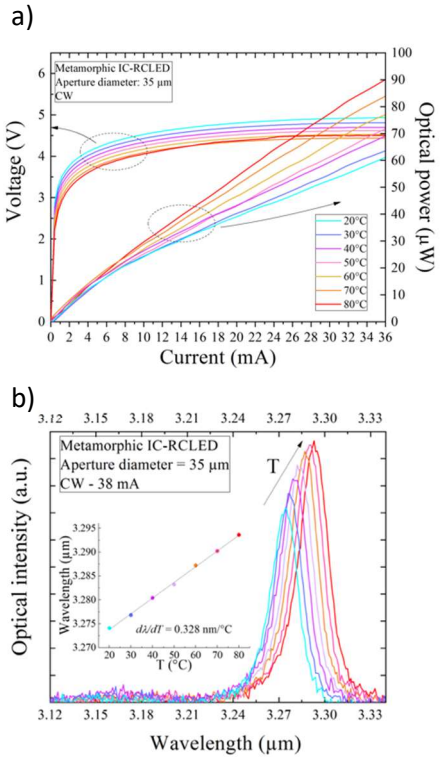

Figure 7 a.) CW P – I – V characteristic and b) electroluminescence spectra for an IC-RCLED with a 35 μm diameter aperture given at different temperatures. Inset shows the temperature dependence of the wavelength. Solid line represents a linear fit to the data.

RCLED and also of the 100 μm IC-LED as well as the simulated reflectivity of the IC-RCLED. If both devices emit at 3.3 μm, the emission of the IC-LED presents a FWHM of 450 nm with a shoulder at lower wavelengths that is not well understood but which has been already observed by others [28]. The IC-RCLED EL spectrum presents a narrow peak at 3.28 μm that matches perfectly with the microcavity resonant mode of the reflectivity spectrum. The FWHM is 20 nm, about 20 times smaller than that of the conventional IC-LEDs.

Figure shows the P-I-V and the electroluminescence (EL) spectra at different temperatures between 20°C and 80°C for an IC-RCLED with a diameter of 35 μm and an injection current of 38 mA. Over the whole measured temperature range (20 – 80°C), the turn-on voltage varies between 4.1 V and 3.5 V, due to

the band gap temperature variation, whereas the series resistance remains essentially constant at ~10 Ω. It is interesting to note that the optical power increases with temperature. For a CW driving current of 36 mA, the output power increases from 60 μW to 90 μW at 20°C and 80°C, respectively. This effect is attributed to a better alignment of with the microcavity resonance [Sarcan F, Nordin M S, Erol A, and Vickers A J 2017 Superlattices and Microstructures, **102** 27-34] as well as maintaining its high quantum efficiency at elevated temperatures. The intensity of the IC-RCLED emission increased with the temperature in the studied range by a factor of ~1.35, while maintaining the same FWHM of ~20 nm. The measured emission linewidth is about 20 times smaller as compared to the conventional IC-LED in the whole studied temperature range. Another advantage of the IC-RCLED is a better temperature stability of the emission wavelength. Indeed, as it is shown on the inset of the Figure , the emission peak linearly increases with a rate of ~0.32 nm/°C, which is considerably lower than the temperature shift those measured for IC-LED [28] and very similarly than other Sb-based VCSELs [13] [10]. Contrary to the IC-LED where the tunability of about 1.37 nm/°C [28] is related to the band gap variation with temperature, in IC-RCLEDs the low tuning rate is due to the slow temperature dependence of the refractive indices of the materials forming the optical cavity. The better temperature stability of the emission wavelength is beneficial to low-cost gas detection sensors where no scanning across the absorption line is required.

3.Conclusions

In summary, we have demonstrated a Mid-IR IC-RCLED combining the benefits of both antimonide and arsenide materials and of their processing technologies. The device emitting near 3.3 μm was grown on a GaSb substrate by MBE and operated in CW regime up to 80°C (setup-limited). An electro-optical lateral confinement was applied within the device structure by wet thermal oxidation of an AlGaAs layer metamorphically grown after the active region. It was demonstrated that this metamorphic layer did not affect the crystal quality of the active region of the device. Thanks to this optimal IC-RCLED configuration combining intracavity electrical injection and lateral confinement, the emission spectral width could be reduced to 20 nm, either a factor of 20 smaller compared to a conventional IC-LED. The narrow

emission line and its weak shift with temperature make this device attractive for low-cost systems for gas analysis.

Acknowledgements

The authors would like to aknowledge the support from the Agence Nationale de la Recherche (ANR-16-CE24-0011); French Program on "Investment for the Future" (Equipex EXTRA, ANR-11-EQPX-0016)

The authors are thankfull for the support from RENATECH (French Network of Major Technology Centers) and RENATECH+ and theirs LAAS-CNRS, Nanorennes and CTM technological facilities.

References

[1]Tournié E, and Cerutti L 2020 *Mid-infrared optoelectronics: materials, devices, and applications*

[2]Vurgaftman I *et al.* 2015 *J. Phys. D: Appl. Phys.* **48**, 123001

[3]Schubert E F, Gessmann T, and J. K. Kim J K 2000 *Kirk-Othmer Encyclopedia of Chemical Technology*, 2000.

[4] Coldren L A, Temkin H, and Wilmsen C W 1999 *Vertical-cavity Surface-emitting Lasers: Design, Fabrication, Characterization, and Applications*. Cambridge University Press

[5]Böttger S, Köhring M, Willer U, and Schade W 2013 *Appl. Phys. B* **113**, 227–232

[6] Schubert E F, Wang Y H, Cho A Y, Tu L W, and Zydzik G J, 1992 *Appl. Phys. Lett.*, **60** 921–923,

[7]Green A M, Gevaux D G, Roberts C, and Phillips C C 2004*Physica E: Low-dimensional Systems and Nanostructures*, **20** 531–535

[8]Grasse C, Wiecha P, Gruendl T, Sprengel S, Meyer R, and Amann M C 2012 *Applied Physics Letters* **101** 221107

[9]Ducanchez A, Cerutti L, Gassenq A, Grech P, and Genty F, *IEEE J. Select. Topics Quantum Electron.* **14** 1014–1021

[10]Al-Saymari F A, Craig A P, Noori Y J, Lu Q, Marshall A R J, and Krier A *Appl. Phys. Lett.* **114** 171103

[11]Bradshaw J L, Bruno J D, Lascola K M, Meissner G P, Pham J T, and Towner F J 2010 *SPIE Defense, Security, and Sensing* **766** 376630C

[12] Arafin S *et al.* 2011 *Opt. Express* **19** 17267

[13] Veerabathran G K, Sprengel S, Andrejew A, and Amann M C 2017 *Appl. Phys. Lett.*, **110** 071104

[14]Sanchez D, Cerutti L, and Tournié E 2012 *Opt. Express* **20** 15540

[15] Laaroussi Y *et al.* 2012 *Electron. Lett.* **48** 1616

[16]H. Gebretsadik H *et al.* 1998 *Electron. Lett.* **34** 3

[17]Jalonen M, Toivonen M, Köngäs J, Salokatve A, and Pessa M 1997 *Electron. Lett.* **33**, 1989

[18]Díaz-Thomas D A *et al.* 2019 *Opt. Express* **27** 31425

[19]Perona A *et al.* 2007 *Semicond. Sci. Technol.* **22** 1140

[20]I. Vurgaftman I *et al.* 2011 *Nat. Commun.* **2** 585

[21]Laaroussi Y, Almuneau G, Sanchez D, and Cerutti L 2011 *J. Phys. D: Appl. Phys.*, **44** 142001.

[22]Bond A E, Dapkus P D, and O'brien J D 1998 *IEEE Photon. Technol. Lett.* **10** 1362

[23]Boucart J, Gaborit F, Fortin C, Goldstein L, Jacquet J, and Leifer K,1999 *Journal of Crystal Growth*, **201–202** 1015.

[24] Deppe D G, Huffaker D L, Oh T H, Deng H, and Deng Q, 1997 *IEEE J. Select. Topics Quantum Electron.* **3** 893

[25] Almuneau G *et al.* 2008 *Semicond. Sci. Technol.* **23** 105021

[26]Ou Y, Gustavsson J S, Westbergh P, Haglund A, Larsson A, and Joel A, 2009 *IEEE Photon. Technol. Lett.* **21** 1840

[27]Dummer M M, Johnson K, Hibbs-Brenner M, and Hogan W K 2012 *SPIE OPTO*, **8276** 82760Y

[28]Kim C S *et al.* 2017 *Opt. Eng*, **57** 1